Optical cuff for optogenetic control of the peripheral nervous system

OPEN ACCESS
IOP Publishing
Journal of Neural Engineering
J. Neural Eng. **15** (2018) 015002 (10pp)
https://doi.org/10.1088/1741-2552/aa9126

Optical cuff for optogenetic control of the peripheral nervous system

Frédéric Michoud[1,2,3], Loïc Sottas[1,2,3], Liam E Browne[2,3,4], Léonie Asboth[5], Alban Latremoliere[2,3], Miyuki Sakuma[2,3], Grégoire Courtine[5], Clifford J Woolf[2,3] and Stéphanie P Lacour[1]

[1] Bertarelli Foundation Chair in Neuroprosthetic Technology, Laboratory for Soft Bioelectronics Interface, Institute of Microengineering, Institute of Bioengineering, Centre for Neuroprosthetics, Ecole Polytechnique Fédérale de Lausanne (EPFL), 1202 Geneva, Switzerland
[2] Department of Neurobiology, Harvard Medical School, Boston, MA 02115, United States of America
[3] FM Kirby Neurobiology Center, Boston Children's Hospital, Boston, MA 02115, United States of America
[4] Wolfson Institute for Biomedical Research, University College London, London WC1E 6BT, United Kingdom
[5] International Paraplegic Foundation Chair in Spinal Cord Repair, Center for Neuroprosthetics and Brain Mind Institute, School of Life Sciences, École Polytechnique Fédérale de Lausanne (EPFL), 1202 Geneva, Switzerland

E-mail: Stephanie.lacour@epfl.ch

Received 29 August 2017, revised 2 October 2017
Accepted for publication 5 October 2017
Published 10 January 2018

Abstract

Objective. Nerves in the peripheral nervous system (PNS) contain axons with specific motor, somatosensory and autonomic functions. Optogenetics offers an efficient approach to selectively activate axons within the nerve. However, the heterogeneous nature of nerves and their tortuous route through the body create a challenging environment to reliably implant a light delivery interface. *Approach.* Here, we propose an optical peripheral nerve interface—an optocuff—, so that optogenetic modulation of peripheral nerves become possible in freely behaving mice. *Main results.* Using this optocuff, we demonstrate orderly recruitment of motor units with epineural optical stimulation of genetically targeted sciatic nerve axons, both in anaesthetized and in awake, freely behaving animals. Behavioural experiments and histology show the optocuff does not damage the nerve thus is suitable for long-term experiments. *Significance.* These results suggest that the soft optocuff might be a straightforward and efficient tool to support more extensive study of the PNS using optogenetics.

Keywords: optogenetics, neural interface, soft materials, optic fiber, peripheral nervous system

Supplementary material for this article is available online

(Some figures may appear in colour only in the online journal)

1. Introduction

Optical neural stimulation is emerging as an exciting and more advantageous alternative to traditional electrical stimulation. The conductive nature of biological tissue leads to electrical current spread, limiting spatial resolution and preventing cell-specific activation (Fenno *et al* 2011, Warden *et al* 2014). Genetic modification of neurons to express opsins, i.e. light-sensitive proteins on neuronal membranes, renders neurons sensitive to light of a specific wavelength with millisecond precision (Boyden *et al* 2005). In the last decade, optogenetics has been used extensively to modulate neural activity in the central nervous system (Deisseroth 2015). In 2016, a human trial of optogenetics to treat retinitis pigmentosa, a

degenerative disease in which the specialized light-sensitive photoreceptor cells in the eye die, was launched (clinicaltrials.gov # NCT02556736).

The use of optogenetics in the peripheral nervous system (PNS) has to date been relatively modest, however, compared to optogenetic control in the brain (Jeschke and Moser 2015, Montgomery *et al* 2016), because of several physiologic and technological challenges. Peripheral nerves are complex, heterogeneous tissues embedded in muscle and connective tissue, which strongly scatter and absorb visible light. Nerves vary significantly in length and diameter, with small visceral nerves 100 times smaller than larger nerves, such as the sciatic nerve. Peripheral nerve stimulation is often conducted in awake, freely moving animals as anesthesia alters nerve excitability properties. Under normal physiologic conditions, peripheral nerves are stretched as joints move and muscles elongate, making consistent light delivery complex. Methods similar to those used in the brain can be used to express opsins in peripheral neurons; however several groups have reported on the difficulties in doing so with sufficient stability and efficacy and without interfering with the regular function of the peripheral neurons (Miyashita *et al* 2013).

Controlled and long-term light delivery to peripheral nerves requires advances in neurotechnology to both enable long-lasting and efficient opsin expression in specific subsets of axons in peripheral nerves and the production of implantable interfaces biointegrated with the flexible nerves and capable of sufficient light power delivery over extended periods of time without producing nerve damage.

In a pioneer study, Llewellyn *et al* demonstrated that optical stimulation of motor units in a nerve of a transgenic mouse expressing the light-activated cation channel ChR2 in $Thy1^+$ neurons better approximated physiological recruitment of motor fibers than electrical stimulation (Llewellyn *et al* 2010). For the first time, this study presented an optoelectronic implant for optical modulation of the sciatic nerve. However, the stiffness of the hybrid implant hosting 16 millimeter-side light emitting diodes (LEDs) limited its application to acute, anaesthetized conditions only.

Transdermal optical stimulation is a non-invasive alternative approach to optogenetic stimulation of peripheral sensory neurons. Excitation (Daou *et al* 2013, Arcourt *et al* 2017, Browne *et al* 2017) and inhibition (Iyer *et al* 2014, Daou *et al* 2016) of mouse primary afferent neurons have been demonstrated using such a design but efficient control of axon activation strongly depends on the optical properties of the intermediate tissues e.g. skin and subcutaneous tissue (Montgomery *et al* 2016, Maimon *et al* 2017). Effectively, stimulation is limited to nerve terminals in the skin whose superficial epidermal layers are innervated by nociceptors. Direct optical stimulation of nerves using an implant is a promising approach for chronic PNS optogenetics. The question is how best to do this? The rapidly expanding use of optogenetics in the CNS has triggered development of a variety of optoprobes in the form of waveguide, miniaturized optical fibers and optoelectronic μLED-based arrays (Wu *et al* 2013, Canales *et al* 2015, Fan and Li 2015, Alt *et al* 2017, Iseri and Kuzum 2017, Pisanello *et al* 2017) yet very few answer the technical needs for chronic peripheral nerve optogenetics.

Inspired by the report from Towne *et al* on an optical fiber-based nerve cuff for optical stimulation in freely-behaving rats (Towne *et al* 2013), we have constructed a soft and biointegrated optocuff as an optical neural implant for chronic peripheral optogenetic stimulation in freely-behaving mice. The optocuff delivers blue light to axons expressing channelrhodopsin (ChR2) in transgenic mice. We overcame chronic implantation challenges with a miniaturized cuff design with soft materials and motion-compliant optic fibers. We demonstrate optical muscle activation with epineural stimulation of Thy1 expressing motor axons and a stable nerve-implant interface after 20 d *in vivo*. This optocuff enables broad optogenetic neuromodulation of peripheral axons and is likely to contribute to the evaluation of using this strategy for new therapeutic interventions for the impaired PNS.

2. Methods

2.1. Mice

All mice were purchased from Jackson Laboratories and Thy1-Cre mice were backcrossed to C57BL/6 for at least five generations. Targeted expression of ChR2-tdTomato was achieved by breeding heterozygous Rosa-CAG-LSL-hChR2(H134R)-tdTomato-WPRE (Ai27D) mice with Thy1-Cre mice. Resultant Thy1-Cre::ChR2 mice were heterozygous for both transgenes and were housed with control littermates. Mice were given *ad libitum* access to food and water and were housed in at 22 $\pm$ 1 °C, 50% relative humidity, and a 12 h light:12 h dark cycle. Male and female mice were pooled by genotype to limit the number of animals used. All experiments were conducted according to institutional animal care and safety guidelines and with IACUC approval at Boston Children's Hospital, and accordance with Swiss federal legislation and under the guidelines established at EPFL and approved by local Swiss Veterinary Offices.

2.2. DRG neuron culture and electrophysiology

Dorsal root ganglia neurons were isolated from adult (3–6 month old) mice and maintained at 37 °C in 5% carbon dioxide. Electrophysiological recordings were made at 20–22 °C up to 24 h after DRG neuron dissociation, using the whole-cell configuration of the patch-clamp technique. Recording pipettes had tip resistances of 4–8 MΩ when filled with (in mM): 135 K-gluconate, 10 KCl, 1 $MgCl_2$, 5 EGTA, and 10 HEPES, pH 7.3. The extracellular solution contained (in mM): 145 NaCl, 5 KCl, 2 $CaCl_2$, 1 $MgCl_2$, 10 HEPES, and 10 glucose, pH 7.4. All solutions were maintained at 300–315 mOsm l^{-1}. Membrane potential was recorded in current clamp mode with an Axopatch 200A amplifier and Digidata 1400A A/D interface using pClamp 10.2 software (Molecular Devices). The data were low-pass filtered at 5 kHz (4-pole Bessel filter) and sampled at 10 kHz. Input resistance was typically >500 MΩ, and cells with resistances <200 MΩ were discarded. Care was

taken to maintain membrane access resistance as low as possible (usually 3–7 MΩ and always less than 10 MΩ). Detailed methods can be found in Browne *et al* (2017).

2.3. Nerve optical properties

Sciatic nerves of five naïve adult mice were carefully explanted after CO_2 asphyxiation, immersed in PBS then embedded in 2.5% agarose gel. Cross-sectional slices (100–1000 μm thick) were obtained with a vibratome apparatus (VTS1200, Leica) and mounted on microscopic glass slides (Superfrost, Thermo Scientific). A drop of saline was added to prevent slices from drying. Tissue transmittance was immediately measured with an optical system composed of a photodiode (S170C, Thorlabs), a power meter console (PM100D, Thorlabs) and a 473 nm DPSS laser (100 mW, LaserGlow) coupled to a multimode SMA optic fiber (105 μm core diameter, 1 m length, Thorlabs). The sensor was shaded with a mask matching nerve cross-section dimensions and a constant intensity (15 $mW \cdot mm^{-2}$) illuminated the slices. The light radial distribution in sciatic nerve tissue was finally modeled using the modified 1D Beer–Lambert law:

$$I(z) = I_0 * e^{(-\mu_{eff} * z)}$$

where I_0 is the optic fiber output irradiance, μ_{eff} the effective attenuation coefficient and z the slice thickness (Al-Juboori *et al* 2013).

2.4. Optocuff construction

The cuff was built upon a polystyrene rod template (0.88 mm diameter, Evergreen). A soft 150 μm thick platinum-catalyzed silicone (Ecoflex 00-50, Smooth-On) was vertically spin-coated and cured (2 h at 80 °C). A gold film was sputtered (80 nm, DP650, Alliance Concept) on the silicone to act as a light reflective coating. Finally, a micrometric film of Polydimethylsiloxane (PDMS) (Sylgard 184, Dow Corning) was used for encapsulation by spray deposition of a PDMS–Heptane mixture. A 12 cm optic fiber (FG105UCA, 105 μm inner core diameter Thorlabs) was processed similarly to previous papers (Sparta *et al* 2011). Briefly, the acrylate coating tip-end of the fiber was dissolved in acetone and terminated with a 1.25 mm ceramic ferrule (CFLC128, Thorlabs). The fiber was then polished using a dedicated kit (Thorlabs) and its light transmission controlled with a power sensor. The distal end of the fiber was perpendicularly coupled to the cuff template and polymer sealed (Kwik-Sil, World Precision Instruments). Finally, the rod was carefully removed, the cuff trimmed (2 mm length, 0.8 mm inner diameter) and a sharp incision was applied transversally to the cuff. The compressive stress built during elastomer curing caused the cuff to spontaneously fold spirally.

2.5. Optocuff implantation

All animal procedures were approved by the institutional animal care and safety guidelines and with IACUC approval at Boston Children's Hospital. Healthy adult (3–6 month old) male and female Thy1-Cre::ChR2 mice of average mass 27.5 g were implanted with the optical cuff. Mice were anesthetized under isoflurane (1–3%) and the body temperature was maintained with a heated surgical table (37 °C). The left hindlimb and head of the mouse were shaved and the skin disinfected using successive applications of betadine and isopropyl alcohol. Under sterile conditions, a skin incision exposed the skull, where 2 precision screws were drilled. The sciatic nerve was exposed at the mid-thigh level after a parallel 1 cm long skin incision and blunt muscles separation. The optical cuff and optic fiber were threaded subcutaneously, the ferrule end laying down the mouse skull and the cuff proximal to the sciatic nerve. A loop was formed on the optic fiber so the cuff has a 90° incidence angle on the sciatic nerve and to relieve the strain along the fiber after implantation. The cuff was then applied to wrap the sciatic nerve and a loose suture secured the optic fiber to surrounding muscles. The separated muscles were sewed back together with absorbable sutures. The ferrule was anchored to the skull with a small amount of dental cement, and the incisions at the head and hindlimb closed with sutures (6-0, Ethicon). Full surgical procedure took 45 min. Control mice used in behavioural experiments underwent similar surgical procedure with the skull and sciatic nerve being exposed. Only a ferrule fixed on a 1 cm long optic fiber was mounted on the skull so blinded experimenters could not distinguish experimental groups. Mice were allowed to recover in single housed cage and subcutaneously injected with post-operative meloxicam analgesic for 3 d.

2.6. EMG electrode implantation and data acquisition

All surgical procedures were performed in accordance with Swiss federal legislation and under the guidelines established at EPFL and approved by local Swiss Veterinary Offices. The animals were administered general anesthesia (mixture of 80 mg ml^{-1} ketamine, 10 mg ml^{-1} xylazine, diluted in saline), using intraperitoneal injections (8.5 ml kg^{-1}). Bipolar intramuscular electrodes (AS632, Cooner Wire) were inserted unilaterally in the tibialis anterior (TA, ankle flexor) muscles to record electromyographic activity. Recording electrodes were created prior to implantation by removing a small part (~200 μm notch) of Teflon insulation. All the wires were connected to a percutaneous amphenol connector (Omnetics Connector Corporation). EMG recordings were synchronized with the laser stimulation onset using a custom-developed Tucker-Davis Technology (TDT) code. Signals were amplified (×1000) and pre-filtered (Bandpass: 100 Hz–1 kHz) with an AM systems amplifier.

2.7. Optogenetic control and high-speed behavioural imaging

The optical cuff was coupled to the laser with a multimode FC/PC optic fiber cable (105 μm core diameter, 2 m length, Thorlabs) using a ceramic mating sleeve (ADAL1, Thorlabs) on the ferrule. It was critical avoiding any physical stress on the mouse during the operation. Mice were housed in a small chamber ($7.5 \times 7.5 \times 15\,cm^3$) chambers and acclimatized for at least 30 min. A counter-balance lever arm (Harvard

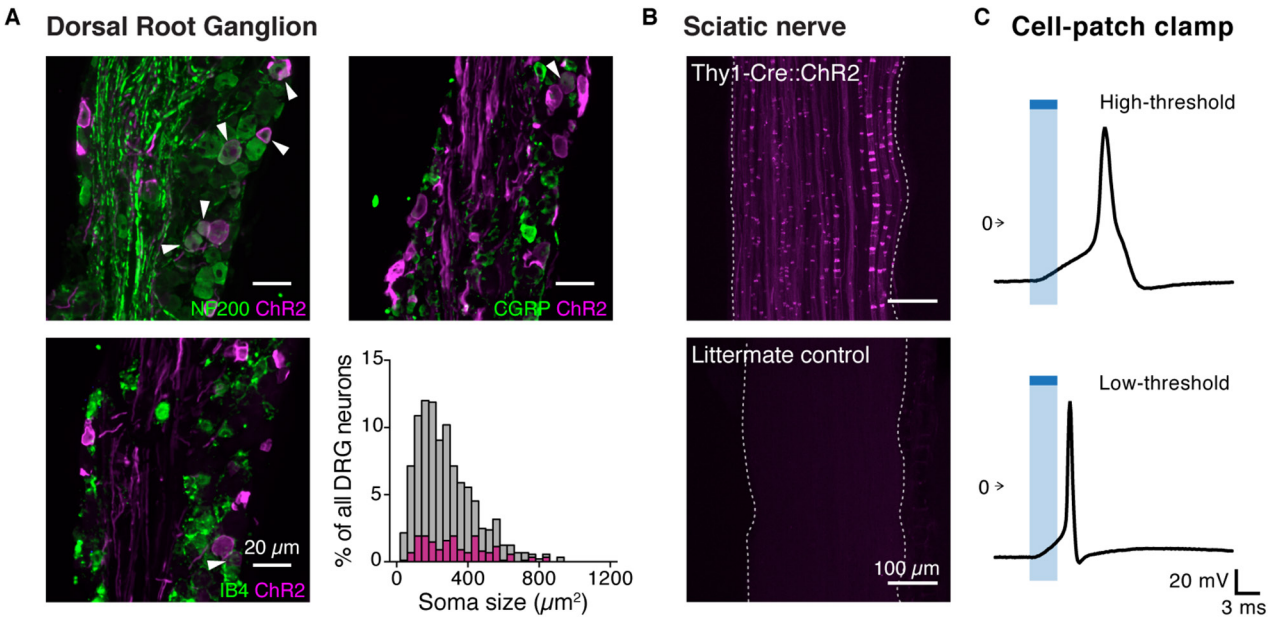

Figure 1. Expression of ChR2 in the PNS of Thy1-Cre::ChR2+ mice. (A) Expression of ChR2-tdTomato in DRG soma was found in a broad class of neurons, myelinated (NF200+ , top left), CGRP+ (top right) and IB4+ (bottom left). White arrows indicate overlapping fluorescence emitting neurons. Scale bar 20 μm. ChR2 was expressed in a wide range of cell sizes as estimated using NeuN+ as a marker for all neurons (bottom right). (B) Expression of ChR2-tdTomato in sciatic nerve fibers. Scale bar 100 μm. Fluorescence was not observed in any of the littermate controls. (C) Whole-cell current clamp recordings of action potentials elicited by light in cultured ChR2-tdTomato+ DRG neurons (17 neurons, 3 mice). These cells displayed a wide range of membrane capacitances and thresholds. Neurons from littermate controls did not show any effect of light (6 neurons). Light (473 nm for 3 ms) applied at 6 mW $\cdot$ mm^{-2}.

Apparatus) relieved the mouse from the laser optic fiber cable weight. A computer-controlled pulse generator (OPTG-4, Doric) was used to supply TTL signals to the laser driver. Simultaneous epineural optogenetic stimulation (average 40 mW laser output) and high-speed recordings were performed. Behaviour was sampled at 1000 frames per second using an acA2040-180kmNIR cameralink CMOS camera (Basler) with a 8 mm lens and set at 500 pixels $\times$ 350 pixels. Acquisition was carried out in LabVIEW on a computer with excess buffer capacity to ensure all frames were successfully retained. Littermate control mice without Cre recombinase and implanted with the optical cuff did not react to blue light pulse (20 ms, 60 mW). Cuff implanted Thy1-Cre::ChR2 mice did not respond to an equivalent off-spectra pulse of light (594 nm, LaserGlow).

2.8. Behavioral experiments

All experiments were conducted in a quiet room at 22 $\pm$ 1 °C with 50% relative humidity. Animals were acclimatized to the behavioral testing apparatus during three habituation sessions in advance of starting the experiment. The behavioral tester was blinded until the experiment was complete.

2.8.1. Mechanical sensitivity. Mice were habituated, single housed in a small transparent chamber (7.5 $\times$ 7.5 $\times$ 15 cm^3) elevated on a wire grid. Mechanical sensitivity was measured by applying an increasing perpendicular force to the lateral plantar surface of the left hindpaw using graded series of six von Frey filaments (with bending force of 0.04, 0.07, 0.16, 0.4, 0.6, 1 g) and counting the number of withdrawal responses across ten applications. The pain mechanical threshold was defined as the minimal force triggering at least five withdrawals.

2.8.2. Thermal sensitivity. Each mouse was habituated on a warmed (29 °C) glass platform of a Hargreave's apparatus (IITC Life Science). Thermal sensitivity was determined by applying a radiant heat source to the plantar hindpaw while measuring the duration before hindpaw withdrawal. The latency for the onset of nocifensive behavior was timed. This latency was determined three times per animal, per session, with a 5 min interval to prevent thermal sensitization.

2.8.3. Dynamic weight bearing. Mice inflammatory pain was assessed using a DWB test (Bioseb). Each mouse was placed 5 min in a Plexiglas chamber (11 $\times$ 19.7 $\times$ 11 cm^3) with a pressure transducers array on the floor. A camera recorded each movement while the mouse was exploring the chamber. Using a software matching pressure data and the video recordings, we discriminated and measured the weight (in grams) applied by the limbs. Finally, we extracted the duration of the cuff implanted hindpaw on the floor over the contralateral one.

2.8.4. Motor sciatic nerve assessment. Motor recovery in mice was assessed using a DigiGait apparatus (Mouse Specifics). Mice were recorded walking on the treadmill videography system at 20 cm s^{-1}. Measures of toe spread (TS) and the print length (PL, distance of the 3rd toe tip to the most posterior paw part) were used to calculate the sciatic nerve functional index (SFI) using the following formula (Baptista *et al* 2007):

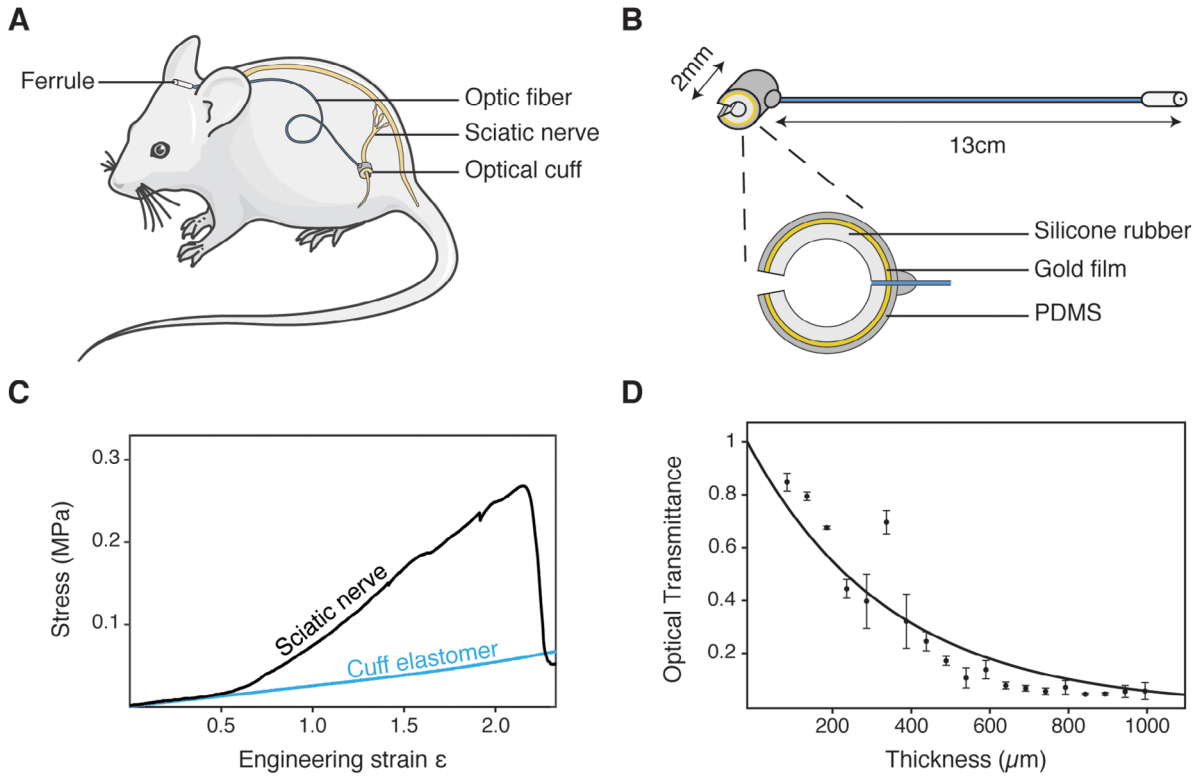

Figure 2. Experimental system for optogenetic activation of the mouse PNS. (A) Optical stimulation carried out epineurally in Thy1-Cre::ChR2 mice implanted with an optocuff. (B) Optical cuff illustration. A thin flexible optic fiber terminates on a silicone rubber-based cuff to deliver an optical stimulation on the mouse sciatic nerve. A gold thin film enables light to reflect internally. (C) Tensile strain-stress curves recorded from a fresh sciatic nerve immersed in physiological conditions and from the elastomeric cuff ($n = 1$ per group). (D) Relative optical power transmission at 473 nm through fresh dissected sciatic nerve tissue ($n = 4$ per thickness).

$$\mathrm{SFI} = 118.9 * \frac{(\mathrm{TS}_{\mathrm{left}} - \mathrm{TS}_{\mathrm{right}})}{\mathrm{TS}_{\mathrm{right}}} 51.2 * \frac{(\mathrm{PL}_{\mathrm{left}} - \mathrm{PL}_{\mathrm{right}})}{\mathrm{PL}_{\mathrm{right}}} 7.5.$$

2.9. Tissue preparation and fluorescence imaging

Mice were anesthetized with pentobarbital (100 mg · kg^{-1} intraperioneal) and fixed by transcardial perfusion with 4% paraformaldehyde dissolved in phosphate buffered saline (PBS). DRG (L3-L5) and sciatic nerves were dissected, post-fixed, washed, cryoprotected with sucrose in PBS (30% w/v) for 2–3 d, and frozen (O.C.T., Tissue-Tek). Cryosections of DRG (10 μm thick) and sciatic nerves (10 μm longitudinal sections, 10 μm cross-sections) were blocked with 1% bovine albumin serum (BSA) and 0.1% triton X-100 in PBS for one hour. Sections were incubated with NF200 (1:2000), CGRP (1:500) primary antibody in fresh blocking solution overnight at 4 °C and washed three times (10 min each) in saline. They were then incubated with secondary IgG antibody (1:500, Life Technologies) for one hour at room temperature, washed three times (10 min each) in PBS, and mounted in Vectashield (H-1200). Fluorescein-conjugated GSL I was used at 1:1000. Finally, sciatic nerve cross-sections were incubated with DAPI (1:1000, 15 min, Sigma) and washed in PBS. DRG and sciatic nerve sections were imaged using a Nikon Eclipse 80i microscope using a Nikon 10× objective and Nikon DS-Qi1MC camera. In DRG and sciatic nerves, fluorescence corresponding to tdTomato was absent in tissues from littermate mice that did not express ChR2-tdTomato or that did not express the Cre recombinase.

3. Results

3.1. Functional expression of ChR2 in the PNS

The light-activated ion channel ChR2 was expressed in a broad class of sensory and motor neurons using a Cre-recombinase transgenic approach (Campsall *et al* 2002); Cre-dependent ChR2-tdTomato mice were crossed with Thy1-Cre driver mice. The resultant Thy1-Cre::ChR2 mice were heterozygous for both transgenes and ChR2 was found in dorsal root ganglion (DRG) neurons and in sciatic nerve axons (figures 1(A) and (B)). Of the ChR2+ DRG neurons, 41% were myelinated (NF200), 4% were CGRP+ and 5% IB4+. Electrophysiological studies using whole-cell current clamp recordings from ChR2-tdTomato+ DRG neurons showed action potentials were elicited by light (figure 1(C)). The large range of membrane capacitances ([11–51] pF; mean 28±4 pF) and thresholds ([−56 to −35] mV; mean −44 ± 2 mV) indicate a broad neuron population was targeted (Browne *et al* 2017), as expected for the Thy1 promoter. Functional expression of ChR2 at the mid-axon enables an epineural light-delivery strategy.

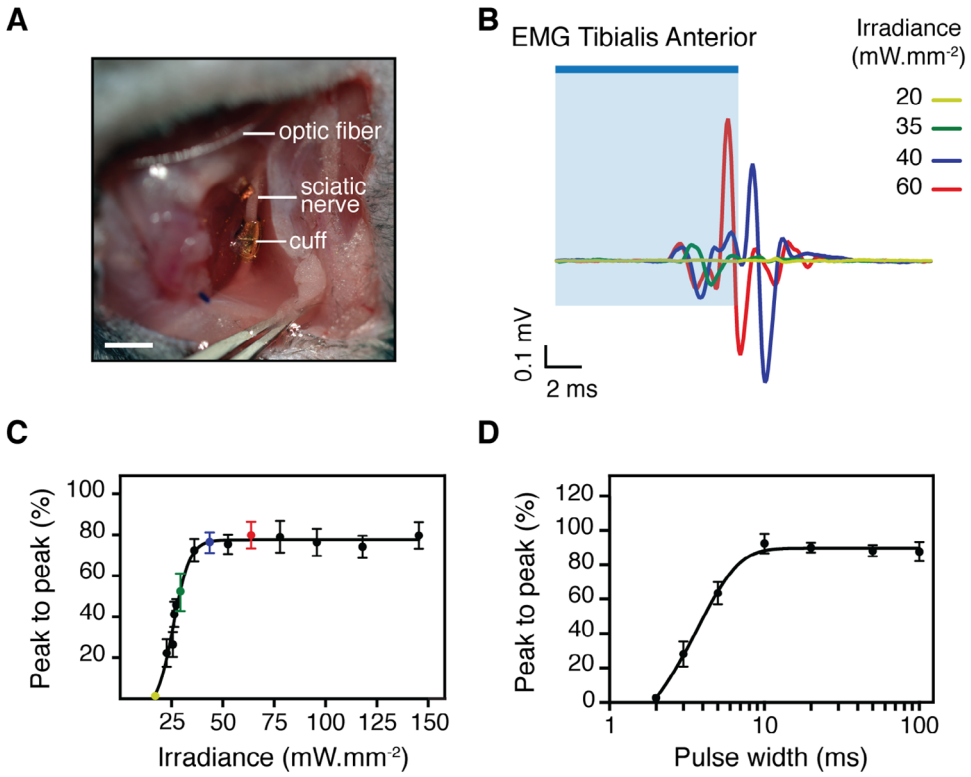

Figure 3. Optical stimulation of the sciatic nerve in anaesthetized mice. (A) Optocuff implantation on the sciatic nerve. Scale bar 2 mm. (B)–(D) Optogenetic stimulation of peripheral axons in anaesthetized Thy1-Cre::ChR2 mice. Light-activated Tibialis Anterior EMG at various stimulation irradiances. The threshold for muscle contraction was 25 mW · mm^{-2} (B). The blue bar indicates the stimulation duration (10 ms). EMG amplitude is directly correlated with stimulation irradiance (C) and pulse width (D). ($n = 3$ Thy1-Cre::ChR2 mice, 5 trials per condition; irradiance set at 60 mW · mm^{-2}).

3.2. A mouse soft, implantable optical cuff

We designed the optocuff as a soft, tubular construct that can be delicately wrapped around a mouse peripheral nerve, e.g. the sciatic nerve (figure 2(A)). Light is delivered to the cuff and the nerve via a flexible optic fiber (105 μm core) subcutaneously threaded from a miniaturized headstage and anchored to the cuff. Multilayers of soft silicones (25 kPa Young's modulus) coated with a reflective thin gold film and a final PDMS film form the 2 mm long, 1 mm diameter cuff (figure 2(B)). The reflective metallic coating limits light spill to the surrounding tissues. The soft implant does not compress nor hinder the natural movement of the nerve as its elasticity surpasses that of the nerve (figure 2(C)).

We measured blue light transmission *in vitro* through slices of freshly dissected sciatic nerves. Light is rapidly absorbed with an effective attenuation coefficient μ_{eff} of 3.503 mm^{-1} at 473 nm tissues (figure 2(D)). We measured an average of 16% optical power losses from the optic fiber to the optocuff such that sufficient light power can be delivered at the optocuff to excite opsin-carrying axons. Heating within the optocuff is limited to photon absorption, a significant advantage compared to LED-based optoelectronic interfaces at analogous optical power (Yizhar *et al* 2011).

3.3. Orderly muscle recruitment to optical stimulation

To measure electromyographic (EMG) responses of anaesthetized Thy1::ChR2 mice to peripheral optical stimulation of motor axons the sciatic nerve of the mouse was exposed and implanted with the optocuff under general anesthesia (figure 3(A)). Then, thin EMG electrodes were inserted into the ipsilateral tibialis anterior (TA), an ankle flexor muscle innervated by the peroneal branch of the sciatic nerve. EMG recordings were synchronized with optical stimulation generated by an external 473 nm laser. Short pulses of light consistently triggered unilateral TA contractions, resulting in light-activated twitches. We characterized the muscle recruitment with the peak-to-peak value of EMG signal in the early phase of the response. We found the muscle fibers were recruited in an orderly fashion with the power of epineural irradiance of the optical stimulation (figures 3(B) and (C)). These results suggest more motor units were recruited with higher irradiance stimulation, consequently inducing larger muscle responses. Latency for the EMG onset (mean 6.1 $\pm$ 0.3 ms, 60 trials, 10 ms pulse width) was stable relative to the optical stimulation intensity and peak-to-peak amplitude (mean 6.1 $\pm$ 0.25 mV), implying direct activation of large and fast motor axons. The TA EMG amplitude directly correlated with optical pulse width (figure 3(D)), indicating an increased activation of motor neurons with longer pulses. These results demonstrate peripheral optogenetic modulation in anesthetized mice with the optocuff.

Next, we tested if the soft optocuff affects the sciatic nerve over time. We implanted a group of Thy1-Cre::ChR2 mice for 20 d with an optocuff wrapped around the left sciatic nerve; one end of the optic fiber was permanently anchored to its head-mounted ferrule. Histological cross-section of the nerve at the cuff site did

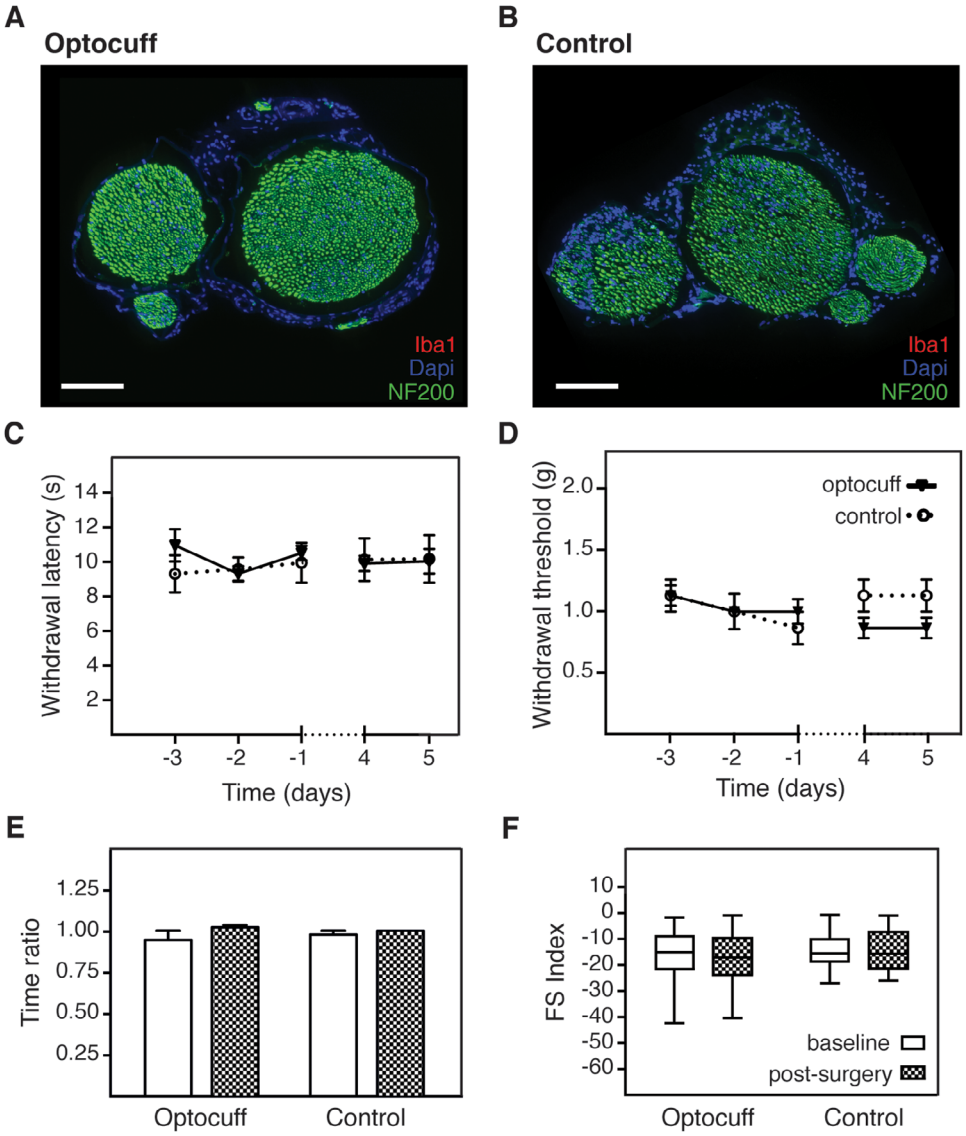

Figure 4. Histology and behavioural experiments reveals the optocuff is suitable for long-term implantation. (A) and (B) Sciatic nerve cross-sectional images 20 d following cuff implantation (A) or sham surgery (B). (C) and (D) Thermal (C) and mechanical (D) sensitivity assessed with Hargreaves and von Frey respectively, in cuff implanted ($n = 6$) and control groups ($n = 3$). Surgery was performed on day 0. (E) Dynamic weight bearing analysis of the duration of time spent on the ipsilateral versus the contralateral hindpaw, before surgery (white) and 5 d post-surgery (optocuff implantation) (grey). (F) Box plot representation of the functional sciatic index calculated gait analysis on treadmill (20 cm s^{-1}).

not show any sign of demyelination or signs of inflammation after the prolonged implantation (figures 4(A) and (B)). Coherent with this, sensory and motor behavioral assessments did not reveal any change at various times after implantation. Thermal and mechanical pain-related assays as well as weight bearing and gait were conducted prior and after surgery and did not reveal any significant change ($p > 0.05$, ANOVA with Dunnett's method).

3.4. Epineural stimulation of motor neuron axons in awake mice

Next, we tested whether the optocuff could reliably deliver epineural optical stimulation in awake, freely-behaving mice. We applied epineurally short (2–100 ms) light pulses at 473 nm with the optocuff while continuously monitoring the behavior of Thy1-Cre::ChR2 mice at 1 kHz with a camera (Basler Ace acA2040-180km). Optogenetic stimulation of the Thy1 axons resulted in short latency hindlimb muscle contraction (figures 5(A) and (B), Supp. V1 (stacks.iop.org/JNE/15/015002/mmedia)). We observed global limb extension and paw opening with short (>5 ms) blue illumination. Probability of behavioural response to optical stimulation was higher with longer pulses (figure 5(C)) and reached 100% for pulses longer than 20 ms. We found the delay for the change in behavior elicited by epineural stimulation was stable through different effective pulse duration (mean 17.9 ± 0.58 ms, figure 5(D)). Using conduction velocity analysis, we concluded these changes in behavior were elicited by direct activation of motor neurons (Steffens *et al* 2012).

Furthermore, absence of response to optical stimulation carried with the optocuff in control littermate mice implies that light-responses were not caused by heat or visual artifact.

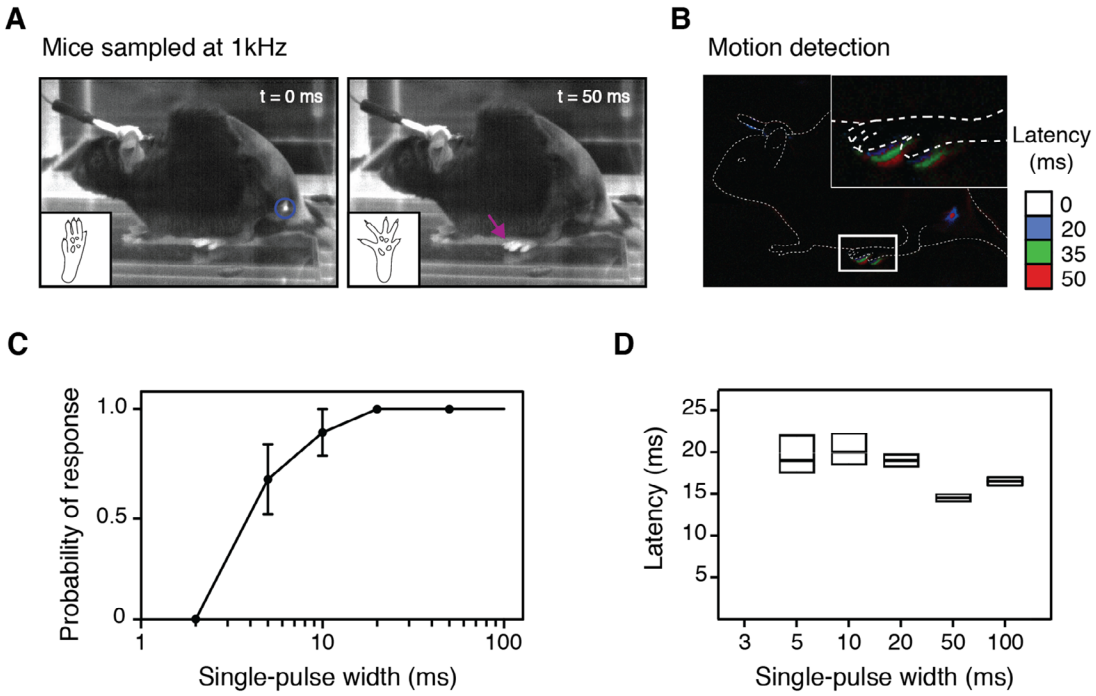

Figure 5. Optogenetic control of peripheral neurons in awake behaving mice. (A) Behaviour sampled at 1 kHz elicited by a single pulse of light (50 ms, 40 mW · mm^{-2}) applied to the sciatic nerve using the optocuff. Onset of the optical stimulation can be seen transdermally. Epineural optical stimulation of Thy1 axons in the sciatic nerve results in hindlimb muscle contraction and paw opening. (B) Motion detection reveals the kinetics of this behaviour. The latency to the response was 17 ms (supplementary video V1). This analysis was conducted by comparing the difference in pixel intensity between frames. (C) Probability of behavioural response to an epineural optogenetic stimulus depends on the pulse width ($n = 3$ mice, 5 trials per condition). (D) Response latency upon epineural activation of Thy1 neurons demonstrates more stability with longer pulses. The mean latency did not depend on pulse duration ($n = 3$ Thy1-Cre::ChR2+ mice, 5 trials per condition). Littermate control cuff implanted mice did not show any response to light stimuli.

4. Discussion

We have developed an implantable optical interface that enables optogenetic modulation of the PNS in freely-behaving small animals such as mice. The soft optocuff can be wrapped around the sciatic nerve inducing minimal foreign body reaction. Using transgenic Thy1-Cre::ChR2 mice, direct and robust muscle activation was obtained by optical stimulation of axons in the sciatic nerve, both in anaesthetized and awake animals. The muscular response can be finely tuned with the optical stimulation parameters i.e. pulse width and irradiance.

Stable light delivery to neurons/axons *in vivo* has been challenging, particularly for applications in the spinal cord or peripheral nerves (Montgomery *et al* 2016). The relative motion of these soft biological tissues prevent long-term and reliable interface with the stiff implants. Although studies have bypassed this problem by stimulating nerve-endings via transdermal illumination (Daou *et al* 2013, Iyer *et al* 2014, Arcourt *et al* 2017, Browne *et al* 2017) or using implanted wireless LEDs (Montgomery *et al* 2015, Park *et al* 2015), interfacing the whole nerve directly offers a broad range of opportunities. We find that reducing the mechanical mismatch between the nerve and implant and optimizing the surgical procedure were key for successful long-term optical coupling with the mouse PNS. The system relies on compliant, subcutaneously tethered fibers that enable a higher intensity and thermally safer light stimulation compared to optoelectronic systems. Additionally, the commercially available external light-sources allow for a large range of solutions for future optogenetic experiments.

Opsin expression in the mouse PNS was achieved using the transgenesis route. Although recent studies have exploited optogenetics in rats or primates (Klein *et al* 2016, Pawela *et al* 2016, L *et al* 2017), mice are still the predominant species used in the neurobiology field. This animal model presents obvious advantages for genetic manipulations, resulting in a large number of Cre-lines and Cre-dependent viral vectors available. We show that ChR2 opsin expression in PNS neurons was robust enough for optical modulation *in vitro* and *in vivo*. The optocuff system can be used for a wide variety of optogenetic experimental approaches, including activation as here and neural inhibition with opsins such as halorhodopsin (NpHr) or archaerhodopsin (Arch). Multi-spectra modulation using multimodal optic fibers will further broaden opportunities for the soft optocuff system (Berndt *et al* 2014, Chuong *et al* 2014).

Finally, long-term selective modulation of the PNS by light delivery offers new experimental opportunities. Optical stimulation of peripheral axons has great implications for muscle control and nerve regeneration (Liske *et al* 2013, Bryson *et al* 2014), for the study of sensory biology (Browne *et al* 2017) and for autonomic output (Kim *et al* 2015). Similarly, optogenetic inhibition *in vivo* will enable to tease out the functional role of specific neurons involve in complex disease mechanisms, such as tactile allodynia following nerve injury (Daou *et al* 2016).

In summary, soft optocuffs are a simple and efficient tool to probe the PNS with optogenetics. Its manufacturing does not require extensive microfabrication processes. Further miniaturization and addition of a wireless head-mounted light source would allow for an even broader use of the implant, especially to study smaller nerves, such as autonomic and visceral nerves (Birmingham *et al* 2014). Finally, the optocuff system supports optogenetics as a versatile tool to unravel the PNS function, an essential step with therapeutic outcomes in many diseases, such as chronic pain.

Acknowledgments

The authors would like to thank I Minev for advice on the soft cuff fabrication, N Andrews for the animal facility management, L Barrett for the laboratory management and G Gorski for his help with histology. Finally, authors would like to thank the EPFL Center for Micronanotechnology (CMi) staff for their technical support. This work is supported by the Swiss National Science Foundation, grant BSCGI0_157800, the Bertarelli Foundation and the European Commission, 329202. The authors have no competing interests to disclose.

Supplementary materials

Video V1: Single-shot optogenetic stimulation of sciatic nerve axons with the behaving mouse sampled at 1 kHz.

ORCID iDs

Frédéric Michoud https://orcid.org/0000-0002-2930-1144

References

Al-Juboori S I, Dondzillo A, Stubblefield E A, Felsen G, Lei T C and Klug A 2013 Light scattering properties vary across different regions of the adult mouse brain *PLoS One* **8** e67626

Alt M T, Fiedler E, Rudmann L, Ordonez J S, Ruther P and Stieglitz T 2017 Let there be light-optoprobes for neural implants *Proc. IEEE* **105** 101–38

Arcourt A, Gorham L, Dhandapani R, Prato V, Taberner F J, Wende H, Gangadharan V, Birchmeier C, Heppenstall P A and Lechner S G 2017 Touch receptor-derived sensory information alleviates acute pain signaling and fine-tunes nociceptive reflex coordination *Neuron* **93** 179–93

Baptista A F, Gomes J R, Oliveira J T, Santos S M, Vannier-Santos M A and Martinez A M 2007 A new approach to assess function after sciatic nerve lesion in the mouse—adaptation of the sciatic static index *J. Neurosci. Methods* **161** 259–64

Berndt A, Lee S Y, Ramakrishnan C and Deisseroth K 2014 Structure-guided transformation of channelrhodopsin into a light-activated chloride channel *Science* **344** 420–4

Birmingham K, Gradinaru V, Anikeeva P, Grill W M, Pikov V, Mclaughlin B, Pasricha P, Weber D, Ludwig K and Famm K 2014 Bioelectronic medicines: a research roadmap *Nat. Rev. Drug Discov.* **13** 399–400

Boyden E S, Zhang F, Bamberg E, Nagel G and Deisseroth K 2005 Millisecond-timescale, genetically targeted optical control of neural activity *Nat. Neurosci.* **8** 1263–8

Browne L E *et al* 2017 Time-resolved fast mammalian behavior reveals the complexity of protective pain responses *Cell Rep.* **20** 89–98

Bryson J B, Machado C B, Crossley M, Stevenson D, Bros-Facer V, Burrone J, Greensmith L and Lieberam I 2014 Optical control of muscle function by transplantation of stem cell-derived motor neurons in mice *Science* **344** 94–7

Campsall K D, Mazerolle C J, De Repentingy Y, Kothary R and Wallace V A 2002 Characterization of transgene expression and Cre recombinase activity in a panel of Thy-1 promoter-Cre transgenic mice *Dev. Dyn.* **224** 135–43

Canales A *et al* 2015 Multifunctional fibers for simultaneous optical, electrical and chemical interrogation of neural circuits *in vivo Nat. Biotechnol.* **33** 277–84

Chuong A S *et al* 2014 Noninvasive optical inhibition with a red-shifted microbial rhodopsin *Nat. Neurosci.* **17** 1123–9

Daou I, Beaudry H, Ase A R, Wieskopf J S, Ribeiro-Da-Silva A, Mogil J S and Seguela P 2016 Optogenetic silencing of Nav1.8-positive afferents alleviates inflammatory and neuropathic pain *eNeuro* **3** 1

Daou I *et al* 2013 Remote optogenetic activation and sensitization of pain pathways in freely moving mice *J. Neurosci.* **33** 18631–40

Deisseroth K 2015 Optogenetics: 10 years of microbial opsins in neuroscience *Nat. Neurosci.* **18** 1213–25

Fan B and Li W 2015 Miniaturized optogenetic neural implants: a review *Lab Chip* **15** 3838–55

Fenno L, Yizhar O and Deisseroth K 2011 The development and application of optogenetics *Annu. Rev. Neurosci.* **34** 389–412

Hernández L F, Castela I, Ruiz-Dediego I, Obeso J A and Moratalla R 2017 Striatal activation by optogenetics induces dyskinesias in the 6-hydroxydopamine rat model of Parkinson disease *Mov. Disord.* **32** 530–7

Iseri E and Kuzum D 2017 Implantable optoelectronic probes for *in vivo* optogenetics *J. Neural Eng.* **14** 031001

Iyer S M, Montgomery K L, Towne C, Lee S Y, Ramakrishnan C, Deisseroth K and Delp S L 2014 Virally mediated optogenetic excitation and inhibition of pain in freely moving nontransgenic mice *Nat. Biotechnol.* **32** 274–8

Jeschke M and Moser T 2015 Considering optogenetic stimulation for cochlear implants *Hear Res.* **322** 224–34

Kim T, Folcher M, Doaud-El Baba M and Fussenegger M 2015 A synthetic erectile optogenetic stimulator enabling blue-light-inducible penile erection *Angew. Chem., Int. Ed.* **54** 5933–8

Klein C, Evrard H C, Shapcott K A, Haverkamp S, Logothetis N K and Schmid M C 2016 Cell-targeted optogenetics and electrical microstimulation reveal the primate koniocellular projection to supra-granular visual cortex *Neuron* **90** 143–51

Liske H, Qian X, Anikeeva P, Deisseroth K and Delp S 2013 Optical control of neuronal excitation and inhibition using a single opsin protein ChR2 *Sci. Rep.* **3** 3110

Llewellyn M E, Thompson K R, Deisseroth K and Delp S L 2010 Orderly recruitment of motor units under optical control *in vivo Nat. Med.* **16** 1161–5

Maimon B E, Zorzos A N, Bendell R, Harding A, Fahmi M, Srinivasan S, Calvaresi P and Herr H M 2017 Transdermal optogenetic peripheral nerve stimulation *J. Neural Eng.* **14** 034002

Miyashita T, Shao Y R, Chung J, Pourzia O and Feldman D E 2013 Long-term channelrhodopsin-2 (ChR2) expression can induce abnormal axonal morphology and targeting in cerebral cortex *Frontiers Neural Circuits* **7** 8

Montgomery K L, Iyer S M, Christensen A J, Deisseroth K and Delp S L 2016 Beyond the brain: Optogenetic control in the spinal cord and peripheral nervous system *Sci. Transl. Med.* **8** 337

Montgomery K L *et al* 2015 Wirelessly powered, fully internal optogenetics for brain, spinal and peripheral circuits in mice *Nat. Methods* **12** 969–74

Park S I *et al* 2015 Soft, stretchable, fully implantable miniaturized optoelectronic systems for wireless optogenetics *Nat. Biotechnol.* **33** 1280–6

Pawela C, Deyoe E and Pashaie R 2016 Intracranial injection of an optogenetics viral vector followed by optical cannula implantation for neural stimulation in rat brain cortex *Methods Mol. Biol.* **1408** 227–41

Pisanello F *et al* 2017 Dynamic illumination of spatially restricted or large brain volumes via a single tapered optical fiber *Nat. Neurosci.* **20** 1180–8

Sparta D R, Stamatakis A M, Phillips J L, Hovelso N, Van Zessen R and Stuber G D 2011 Construction of implantable optical fibers for long-term optogenetic manipulation of neural circuits *Nat. Protocols* **7** 12–23

Steffens H, Dibaj P and Schomburg E D 2012 *In vivo* measurement of conduction velocities in afferent and efferent nerve fibre groups in mice *Physiol. Res.* **61** 203–14

Towne C, Montgomery K L, Iyer S M, Deisseroth K and Delp S L 2013 Optogenetic control of targeted peripheral axons in freely moving animals *PLoS One* **8** e72691

Warden M R, Cardin J A and Deisseroth K 2014 Optical neural interfaces *Annu. Rev. Biomed. Eng.* **16** 103–29

Wu F, Stark E, Im M, Cho I J, Yoon E S, Buzsaki G, Wise K D and Yoon E 2013 An implantable neural probe with monolithically integrated dielectric waveguide and recording electrodes for optogenetics applications *J. Neural Eng.* **10** 056012

Yizhar O, Fenno L E, Davidson T J, Mogri M and Deisseroth K 2011 Optogenetics in neural systems *Neuron* **71** 9–34